This article has been accepted for publication in a future issue of this journal, but has not been fully edited. Content may change prior to final publication. Citation information: DOI 10.1109/LAWP.2015.2403237, IEEE Antennas and Wireless Propagation Letters

A Correlation Model for Non-Stationary Time-Variant On-Body Channels

Oudomsack Pierre Pasquero[1,2], Ramona Rosini[1,3], Raffaele D'Errico[1,2], Claude Oestges[4]
[1]CEA, LETI, Minatec Campus, France - oudomsackpierre.pasquero@cea.fr, raffaele.derrico@cea.fr
[2]Univ. Grenoble-Alpes, Grenoble, France
[3]DEI, University of Bologna, Italy - ramona.rosini@unibo.it
[4]ICTEAM, Université Catholique de Louvain, Louvain-la-Neuve, Belgium - claude.oestges@uclouvain.be

***Abstract*—The temporal variation of spatial correlation between on-body radio links are empirically characterized for different walking scenarios. Non-stationary behaviors are highlighted and a model is proposed for the long-term fading correlation.**

***Index Terms*—Body Area Networks, channel modeling, correlation, measurement.**

I. Introduction

Body Area Networks (BANs) consist of different wireless nodes placed on or in the proximity of the human body. BAN applications encompass various domains such as medicine, surveillance, sport and entertainment [1]. In the last years, significant efforts have been made in BAN radio channel modeling. In particular, the first- and second- order characteristics were investigated in static and dynamic conditions [2]–[6]. It has been observed that the communication reliability is strongly affected by second-order statistics. To overcome the strong attenuation and shadowing by the human body, relay approaches have been proposed [7]. However, the design and performance evaluation of multi-hop techniques is highly dependent on the correlation between different links. In [8]–[10], on-body correlations have been modeled assuming stationary statistics over time. Even if this might be true for small periods of time and regular motions, this might not be valid for realistic motions.

In this letter, we investigate the inter-link correlation properties of on-body channels in various walking scenarios with a focus on the non-stationary effects. In [5] the authors modeled the BAN failures with a semi Markov-chain Model. Here the same approach is used but to describe the non-stationary behaviour of WBAN channels, and model the changing spatial correlation properties along the body movement.

II. On-Body channel measurement campaigns

On-body channel measurement campaigns were performed with several human subjects in different indoor environments for various mobility scenarios. To compare the results obtained from different measurement campaigns, we focus on datasets recorded at 4.2 GHz, and selected the measurements performed with antennas presenting normal polarization with respect to the body surface. The main difference between both datasets lie in the observation duration and the non-regular mobility pattern in [4].

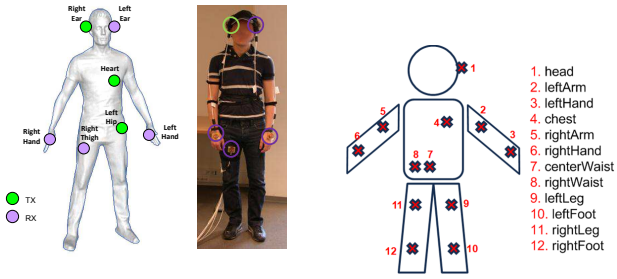

(a) (b)

Fig. 1. On-body nodes emplacements in *Measurement Campaign I* (a) and *Measurement Campaign II* (b)

A. Measurement Campaign I

This ultra-wideband measurement campaign was previously exploited at 2.4 GHz in [11]. Here, we rather exploit the channel acquisitions at 4.2 GHz, in order to compare them with those presented in the next subsection.

The measurement testbed consisted in a pulse step generator and a power amplifier at the transmitting side, whereas low-noise amplifiers were connected to a wideband real-time digital oscilloscope at the receiving side. This configuration enabled the simultaneous collection of several impulse responses, each one corresponding to a different on-body link. Fig. 1(a) depicts the different transmitter and receiver locations considered. Wideband Top Loaded Monopole (TLM) antennas were used. TLM is based on a wire-patch monopole design [12] and is fed by a stripline within the antenna ground plane. TLMs present an impedance matching band from 2.33 up to 11 GHz, with respect to $S_{11} < -7$ dB, with a total on-body efficiency of 70% from 2.36 to 5 GHz. The experiments were performed in an indoor office equipped with some general furniture. Three human subjects walking on a straight line were considered. For every subject, two acquisitions of 3 s each were performed. The sampling period considered in this data is equal to 20 ms. Hereafter, we number the human subjects of this measurement campaign from 1 to 3, and we denote *walk* 1 and *walk* 2 the two measurements performed for each subject.

This article has been accepted for publication in a future issue of this journal, but has not been fully edited. Content may change prior to final publication. Citation information: DOI 10.1109/LAWP.2015.2403237, IEEE Antennas and Wireless Propagation Letters

B. Measurement Campaign II

In this measurement campaign, a MIMO 8×8 Elektrobit channel sounder was used to characterize the on-body radio channel [4]. Each on-body node was connected to the channel sounder through a 6 m SMA cable. Different configurations were considered resulting into 12 node positions on the body (Fig. 1(b)). SMT-3TO10M-A SkyCross antennas placed normally to the body were employed in the measurements. The channel burst sample rate was about 20 Hz. Each burst consisted of 4 successive measurements that were averaged to increase the measurement Signal-to-Noise Ratio (SNR). Eventually, the effective sampling period was equal to 23.6 ms. Measurements were taken successively on two subjects, namely subjects 4 and 5, walking freely in a quasi-empty room. For each acquisition, 3000 channel measurements were recorded, corresponding to about 18 s for each dataset.

III. Fading correlation

In the received signal power, one can distinguish long-term and short-term fading components as outlined by:

$$P(t) = P_0 \cdot L(t) \cdot S(t) \tag{1}$$

where P_0 represents the mean received power, while $L(t)$ and $S(t)$ are the normalized long- and short-term fading components, respectively. It has been shown that the long-term fading is related to the shadowing by the human body during the movements [10]. This effect is particularly evident in walking scenarios when one of the antenna is placed on a limb [4], [10]. In the sequel, we extract the normalized long-term fading component from the measurements by applying a low pass filter. In practice, the filtering is realized by averaging the time-dependent power transfer function $P(t)$ with a sliding time window of duration Δt:

$$L(t) = \frac{1}{\Delta t} \int_{t-\Delta t/2}^{t+\Delta t/2} \frac{P(t)}{P_0} dt. \tag{2}$$

The window width Δt is equal to 320 ms and 330.4 ms for measurement campaign *(MC)-I* and *-II* respectively. The window widths difference is due to the different sampling periods used for each measurement campaign. Moreover, a division by the mean received power P_0 is made for power normalization.

Fig. 2 and Fig. 3 illustrate examples of long-term fading extraction for two given on-body links in *MC-I* and *MC-II* respectively. The long-term fading has been found to follow a log-normal distribution. Hence, we define the inter-link correlation on the long-term fading (expressed in dB) as follows:

$$\rho_{i,j}(t\,;\,T_{\text{obs}}) = \frac{\mathbb{E}\left[\left(L_{\text{TX},i} - \mathbb{E}\left[L_{\text{TX},i}\right]\right)\left(L_{\text{TX},j} - \mathbb{E}\left[L_{\text{TX},j}\right]\right)\right]}{\sqrt{\mathbb{E}\left[L_{\text{TX},i}^2 - \mathbb{E}^2\left[L_{\text{TX},i}\right]\right]\mathbb{E}\left[L_{\text{TX},j}^2 - \mathbb{E}^2\left[L_{\text{TX},j}\right]\right]}} \tag{3}$$

where $\mathbb{E}[.]$ is the expectation operator over an observation window T_{obs}. $L_{\text{TX},i}$ and $L_{\text{TX},j}$ represent the long-term fading components in dB of the radio links associated to the same transmitting antenna position *TX* and the receiving antenna positions i and j respectively. More in detail, the correlation value obtained at the instant t is computed from the long-term fadding measured during the window time $[t - T_{\text{obs}}/2\ ;\ t + T_{\text{obs}}/2]$. For t higher than $(T_{meas} - T_{obs}/2)$, the higher bound of the window is set to T_{meas}, i.e. 3s for *MC-I* and 18s for *MC-II*. The lower bound is not modified and still set to $(t - T_{\text{obs}}/2)$.

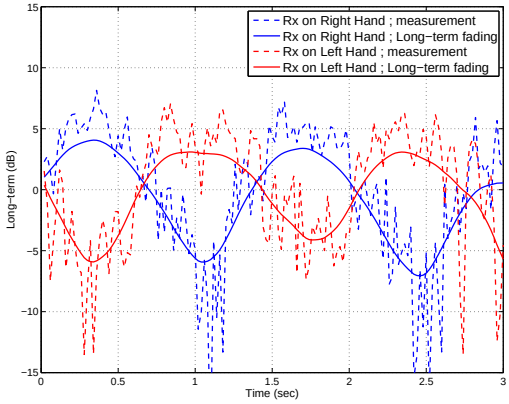

Fig. 2. *MC-I* - Long-term fading extraction $\Delta t = 320$ ms - *subject* 1 - *walk* 2 - Tx on Heart

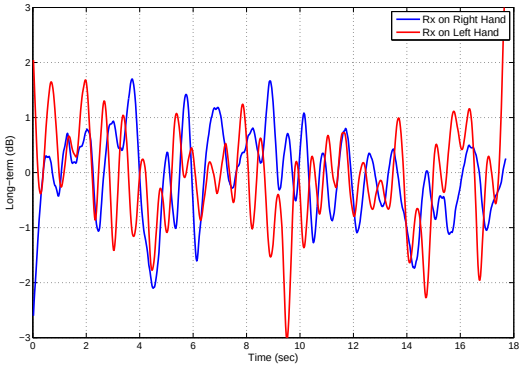

Fig. 3. *MC-II* - Long-term fading extraction $\Delta t = 330.4$ ms - *subject* 4 - Tx on Heart

IV. Results

A. Correlation Dynamics

According to the node location and the human body motion, long-term fading patterns related to different links can be synchronous or asynchronous. For instance, in very regular walks as the one shown in Fig. 2, the Heart-Right Hand and Heart-Left Hand links exhibit anti-correlated fading behaviors because of the regular swinging of the arms. This pattern is expected to result in high anti-correlation values (typically smaller than -0.4).

In a previous work, it has been shown that the correlation computed on different time-blocks can have different values [13]. Let us now compute the long-term fading correlation over a sliding observation time window. The window width T_{obs} has been empirically chosen by visual inspection of the channel data. This value has been chosen in order to be smaller than the total duration of the observation, i.e. 3 s in *MC-I*, and several time larger than the expected correlation time in the on-body indoor walking channels (typically from 20 ms up to

This article has been accepted for publication in a future issue of this journal, but has not been fully edited. Content may change prior to final publication. Citation information: DOI 10.1109/LAWP.2015.2403237, IEEE Antennas and Wireless Propagation Letters

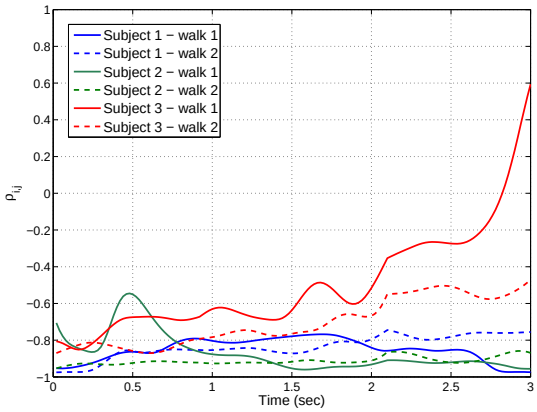

Fig. 4. *MC-I* - $\rho_{i,j}$ over $T_{\text{obs}} = 1.8$s - Tx on Heart and Rxs on Left/Right Hand

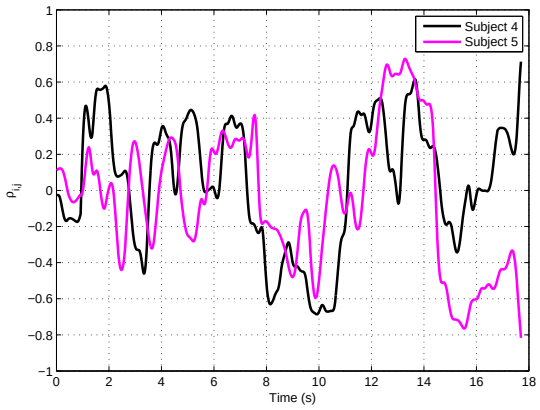

Fig. 5. *MC-II* - $\rho_{i,j}$ over $T_{\text{obs}} = 1.8$s - Tx on Heart and Rxs on Left/Right Hand

100 ms according to the link [14] [15]). Fig. 4 and Fig. 5 show the correlation values measured in both sets of measurements.

In Fig. 4, the two radio links are highly anti-correlated for all subjects and walk cycles. This is consistent with the behavior of the extracted long-term fading components given in Fig. 2. This anti-correlation characteristic can be easily interpreted by the fact that since one node is located on the heart, both radio links are shadowed by the body alternately [10]. The correlation characteristics are relatively stable over time, except for *walk* 1 of *subject* 3, where the increase of $\rho_{i,j}$ during the last second is due to the fact that the subject finished the walk prematurely.

By contrast, Fig. 5 shows that the correlation values strongly vary over time in *MC-II*. This is in line with the long-term fading pattern variations shown in Fig. 3. When the subjects are let free to move and do not follow a straight path, the limb swinging is more random and changes during the movement. Moreover, the proximity with some objects in the environment could yield to very slow variations of the long-term fading that are included in the shadowing contributions.

Although both measurement campaigns have been performed in walking scenarios, the space-time correlation characteristics are totally different. This correlation analysis shows a non-stationary behavior of the channel in general walking scenarios, i.e. not in particular scenarios such as walks on a straight line. The correlation characteristics depend on the observation instant t as showed in Fig. 5. This analysis confirms the observation of non-stationary on-body channel characteristics outlined in [16].

B. Correlation modeling

In order to model the on-body channel space-time correlation properties over several seconds in random walking scenarios, we exploit the results obtained with *MC-II*. We propose to use a Markov chain defined by 5 correlation states (see Fig. 6):

- highly anti-correlated (HA): $\rho_{i,j} \leq -0.5$
- anti-correlated (A): $-0.5 < \rho_{i,j} \leq -0.3$
- non-correlated (D): $-0.3 < \rho_{i,j} < 0.3$
- correlated (C): $0.3 \leq \rho_{i,j} < 0.5$

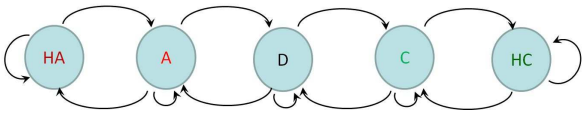

Fig. 6. Space-time correlation model based on a Markov chain

- highly correlated (HC): $0.5 \leq \rho_{i,j}$.

The correlation threshold values are arbitrary chosen considering the correlation values obtained in *MC-II*. And we assign the following correlation values for each correlation state:

- highly anti-correlated (HA): $\rho_{i,j} = -0.6$
- anti-correlated (A): $\rho_{i,j} = -0.4$
- non-correlated (D): $\rho_{i,j} = 0$
- correlated (C): $\rho_{i,j} = 0.4$
- highly correlated (HC): $\rho_{i,j} = 0.6$.

We compute the transition probabilities between all states according to Fig. 6. Let us remind that the sampling period is equal to 23.6 ms in *MC-II*. We intuitively understand that these transition probabilities are strongly dependent on the sampling period. Indeed, the greater the duration between two consecutive observation instants (i.e. the sampling period), the higher the probability for the correlation state to change. In our case, we note that the sampling period is small enough to not allow any brutal correlation value variation. In other words, between two consecutive observation instants, there is not any transition from a correlation state to another one which is very different.

The transition probability values are found to be very similar between the subjects. The mean values over *subject* 4 and *subject* 5 are reported in Table I for different on-body link pairs. We remark that the highest transition probabilities are those for which there is no transition from a correlation state to a different one. This means that the channel correlation characteristics are stable between two consecutive observation instants, i.e. during one sampling period (23.6 ms).

In order to initialize the Markov process, starting probabilities are required. For that purpose, we compute the probabilities for all radio link pairs in each correlation state. Comparing the obtained values given in Table II, one can see that most of them are different between the two subjects. This difference

This article has been accepted for publication in a future issue of this journal, but has not been fully edited. Content may change prior to final publication. Citation information: DOI 10.1109/LAWP.2015.2403237, IEEE Antennas and Wireless Propagation Letters

TABLE I
TRANSITION PROBABILITIES BETWEEN THE CORRELATION STATES

Tx location	Heart	Right Hip	Hip center	Left Ear
Rxs locations	Left/Right Hand	Left/Right Hand	Left/Right Foot	Left/Right Hand
$P(\text{HA} \rightarrow \text{HA})$	0.97	0.97	0.95	0.97
$P(\text{HA} \rightarrow \text{A})$	0.03	0.03	0.05	0.03
$P(\text{A} \rightarrow \text{HA})$	0.03	0.02	0.07	0.08
$P(\text{A} \rightarrow \text{A})$	0.92	0.92	0.83	0.86
$P(\text{A} \rightarrow \text{D})$	0.05	0.06	0.10	0.07
$P(\text{D} \rightarrow \text{A})$	0.01	0.01	0.01	0.01
$P(\text{D} \rightarrow \text{D})$	0.97	0.96	0.96	0.98
$P(\text{D} \rightarrow \text{C})$	0.2	0.03	0.02	0.01
$P(\text{C} \rightarrow \text{D})$	0.06	0.09	0.06	0.04
$P(\text{C} \rightarrow \text{C})$	0.92	0.87	0.89	0.90
$P(\text{C} \rightarrow \text{HC})$	0.02	0.04	0.04	0.06
$P(\text{HC} \rightarrow \text{C})$	0.04	0.02	0.05	0.04
$P(\text{HC} \rightarrow \text{HC})$	0.96	0.98	0.95	0.96

TABLE II
INITIAL CORRELATION STATE PROBABILITIES

Tx location	Heart	Right Hip	Hip center	Left ear
Rxs locations	Left/Right Hand	Left/Right Hand	Left/Right Foot	Left/Right Hand
Subject 4 - $P(\text{HA})$	0.10	0.00	0.03	0.31
$P(\text{A})$	0.10	0.02	0.02	0.13
$P(\text{D})$	0.50	0.15	0.42	0.40
$P(\text{C})$	0.24	0.13	0.11	0.13
$P(\text{HC})$	0.06	0.70	0.42	0.03
Subject 5 - $P(\text{HA})$	0.14	0.19	0.22	0.15
$P(\text{A})$	0.12	0.15	0.09	0.04
$P(\text{D})$	0.59	0.55	0.45	0.42
$P(\text{C})$	0.06	0.06	0.21	0.08
$P(\text{HC})$	0.09	0.05	0.03	0.31

is related to the fact that the subjects have a different walking behavior. In the model implementation, the initialization phase of the correlation states can alternate between these two sets of probabilities corresponding to different walking modes.

V. CONCLUSIONS

In this letter, we characterized space-time correlation properties of on-body radio links. It is observed that the correlation properties could vary from very stationary to non stationary according to the observation time and regularity of walk. A Markov chain model has been proposed to reproduce the variation over time of the space-time correlation. This model can be exploited for cooperative approaches using on-body nodes as relays.

ACKNOWLEDGMENT

This work was carried out in the framework of a short term scientific mission of Claude Oestges to CEA-LETI, jointly funded by COST Action IC1004 and the Belgian Fonds de la Recherche Scientifique. Work by UCL was found by the Interuniversity Attraction Poles Programme 7/23 BESTCOM initiated by the Belgian Science Policy Office. Work by CEA-LETI has been partially funded by the French ANR project CORMORAN. This publication was made possible by NPRP grant [6-1508-2-616] from the Qatar National Research Fund (a member of Qatar Foundation). The statements made herein are solely the responsibility of the authors.

REFERENCES

[1] H. Cao, V. Leung, C. Chow, and H. Chan, "Enabling technologies for wireless body area networks: A survey and outlook," *Communications Magazine, IEEE*, vol. 47, no. 12, pp. 84 –93, dec. 2009.

[2] M. Kim and J.-i. Takada, "Statistical model for 4.5-GHz narrowband on-body propagation channel with specific actions," *Antennas and Wireless Propagation Letters, IEEE*, vol. 8, pp. 1250–1254, 2009.

[3] S. Cotton, G. Conway, and W. Scanlon, "A time-domain approach to the analysis and modeling of on-body propagation characteristics using synchronized measurements at 2.45 GHz," *Antennas and Propagation, IEEE Transactions on*, vol. 57, no. 4, pp. 943 –955, april 2009.

[4] S. van Roy, F. Quitin, L. Liu, C. Oestges, F. Horlin, J. Dricot, and P. De Doncker, "Dynamic channel modeling for multi-sensor body area networks," *Antennas and Propagation, IEEE Transactions on*, vol. 61, no. 4, pp. 2200–2208, 2013.

[5] S. Wang and J.-T. Park, "Modeling and analysis of multi-type failures in wireless body area networks with semi-markov model," *Communications Letters, IEEE*, vol. 14, no. 1, pp. 6–8, January 2010.

[6] X. Yang, S. Yang, Q. Abbasi, Z. Zhang, A. Ren, W. Zhao, and A. Alomainy, "Sparsity-inspired non-parametric probability characterization for radio propagation in body area networks," *Biomedical and Health Informatics, IEEE Journal of*, vol. PP, no. 99, pp. 1–1, 2014.

[7] P. Ferrand, J.-M. Gorce, and C. Goursaud, "On the packet error rate of correlated shadowing links in body-area networks," in *Proceedings of the 5th European Conference on Antennas and Propagation (EUCAP)*,, 2011, pp. 3094–3098.

[8] L. Liu, P. De Doncker, and C. Oestges, "Fading correlation measurement and modeling on the front side of a human body," in *3rd European Conference on Antennas and Propagation, 2009. EuCAP 2009.*, 2009.

[9] X. D. Yang, Q. Abbasi, A. Alomainy, and Y. Hao, "Spatial correlation analysis of on-body radio channels considering statistical significance," *IEEE Antennas and Wireless Propagation Letters*, vol. 10, pp. 780–783, 2011.

[10] R. D'Errico and L. Ouvry, "A statistical model for on-body dynamic channels," *International Journal of Wireless Information Networks*, vol. 17, pp. 92–104, 2010, 10.1007/s10776-010-0122-0. [Online]. Available: http://dx.doi.org/10.1007/s10776-010-0122-0

[11] R. Rosini and R. D'Errico, "Comparing on-body dynamic channels for two antenna designs," in *Antennas and Propagation Conference (LAPC), 2012 Loughborough*, 2012, pp. 1–4.

[12] C. Delaveaud, P. Leveque, and B. Jecko, "New kind of microstrip antenna: The monopolar wire-patch antenna," *Electronics letters*, vol. 30, no. 1, pp. 1–2, 1994.

[13] O. P. Pasquero, R. Rosini, R. D'Errico, and C. Oestges, "On-Body Channel Correlation in Various Walking Scenarios," in *8th European Conference on Antennas and Propagation, 2014. EuCAP 2014.*, 2014.

[14] R. Rosini, "From radio channel modeling to a system level perspective in body-centric communications," Ph.D. dissertation, University of Bologna, May 2014.

[15] L. Liu, "Cooperative wireless channel characterization and modeling: Application to body area and cellular networks," Ph.D. dissertation, Catholic University of Leuven, March 2012.

[16] V. Chaganti, L. Hanlen, and D. Smith, "Are narrowband wireless on-body networks wide-sense stationary?" *Wireless Communications, IEEE Transactions on*, vol. 13, no. 5, pp. 2432–2442, May 2014.